Available online at www.sciencedirect.com
ScienceDirect
Trans. Nonferrous Met. Soc. China 23(2013) 1639−1645
Transactions of Nonferrous Metals Society of China
www.tnmsc.cn

Microstructure and formation mechanism of Ni−Al intermetallic compounds fabricated by reaction synthesis

Hong-zhi CUI, Na WEI, Liang-liang ZENG, Xiao-bin WANG, Hua-jie TANG

School of Materials Science and Engineering, Shandong University of Science and Technology, Qingdao 266590, China

Received 2 February 2013; accepted 7 May 2013

Abstract: Ni−Al intermetallic compounds from Ni and Al powder were obtained by thermal explosion. Effects of molar ratio of Ni to Al in raw materials on the phases, microstructures and microhardness of the final products were studied. The results show that a single phase of NiAl is obtained with the composition corresponding to n(Ni):n(Al)=1:1. However, when the molar ratio of Ni to Al increases to 2:1, the product is composed of Ni_3Al and NiAl, in which NiAl phase is in the majority with an irregular morphology and Ni_3Al is in the minority mainly along the grain boundary of the NiAl. As the molar ratio of Ni to Al continues to increase to 3:1, the microstructures of the product are diversified. Lots of M-NiAl with needle-like or long lathing shape and many γ'-Ni_3Al with irregular and pointed strip-like morphology even appear besides β-NiAl with dendritic structure, γ-Ni_3Al with irregular or net-like morphology because of the non-equilibrium cooling and large difference in composition of β-NiAl.
Key words: intermetallic compounds; Ni−Al; reaction synthesis; microstructure

1 Introduction

Ni−Al alloys are well known as high temperature structural materials due to their low density, high melting point, good thermal conductivity, excellent acid/alkali corrosion resistance as well as good oxidation resistance at elevated temperatures. The major intermetallic compounds of Ni−Al alloys are NiAl and Ni_3Al [1−3]. So far, the Ni−Al alloys have been applied to heat shields for combustion chambers and gas turbines etc [4−6].

Ni−Al intermetallic compounds have been prepared by a variety of methods including powder metallurgy [7], casting [8], rapid solidification [9,10], mechanical alloying [11,12], sintering [13], combustion synthesis etc [14−17]. SUN et al [9] studied the composition and morphology of NiAl intermetallic compounds with different Ni contents. The results showed that the products had B2 structure and the morphology of $Ni_{0.53}Al_{0.47}$ was equiaxed crystal whereas 0.56−0.60 Ni was irregular and regular columnar crystals. In the study of PABI and MURTY [11], nanocrystalline $NiAl_3$, NiA1 and Ni_3A1 phases were synthesized by mechanically alloying. In addition, the study of RUIZ-LUNA et al [12] revealed that the microstructural transformation mechanism of B2-NiAl during mechanical alloying process was Ni+Al → $NiAl_3$ → Ni_2Al_3 → NiAl. However, DONG et al [13] deduced that the microstructure transformation process of NiAl during pressless sintering process was Ni+Al→Ni_2Al_3→NiAl →Ni_3Al.

Combustion synthesis (CS) offers an efficient and attractive method for preparation of ceramics, intermetallics and their composites with the advantages of simple process, high efficiency and low cost etc [14]. BISWAS and ROY [15] studied the evolution of the structure and the mechanism of NiAl prepared by CS. The morphologies of the intermediate phases, such as $NiAl_3$ and Ni_2Al_3, were observed. Moreover, the equiaxed grains of NiAl and the lath-like NiAl martensite which was a Ni-rich phase were also obtained. In order to investigate the microstructural evolution of Ni_3Al intermetallic from Al and Ni powders (1:1) during the CS, a combustion front quenching method (CFQM) was used by FAN et al [16]. The experimental results showed that the microstructure of the Ni droplet was composed of parallel lath-like M-NiAl phase in the surface region and γ'-Ni_3Al phase in the central region.

Foundation item: Projects (51072104, 51272141) supported by the National Natural Science Foundation of China; Project (ts20110828) supported by Taishan Scholars Project of Shandong Province, China; Project (BS2010CL038) supported by the Research Award Fund for Outstanding Young and Middle-aged Scientists of Shandong Province, China
Corresponding author: Hong-zhi CUI; Tel: +86-532-86057929; E-mail: cuihongzhi1965@163.com
DOI: 10.1016/S1003-6326(13)62642-4

In addition, a dissolution–precipitation mechanism of the combustion synthesis of NiAl was proposed. However, ZHU et al [17] studied the reaction process of a multilayer Ni/Al system based on precise temperature measurements and analyzed the evolvement of microstructure in quenched samples.

As different phases and microstructures of Ni−Al alloys can be obtained even by the same methods and ratios of the raw materials, it is necessary to analyze the microstructures and formation mechanism in different proportions of Ni to Al. In this study, Ni−Al intermetallic compounds were fabricated by high speed combustion synthesis, i.e. thermal explosion reaction synthesis mode. Simultaneously, the effects of molar ratios on the phase constitution, microstructure and microhardness were explored though investigating the phase transformation and morphological features of the products, in order to provide useful data for improving the mechanical performance of Ni−Al alloys.

2 Experimental

The raw materials used in this experiment were Ni powder (99.0% purity, <38 μm particle size) and Al powder (99.0% purity, 38−50 μm particle size). The SEM micrographs of reactant powders are shown in Fig. 1. The size of Al powder was a little larger than that of Ni powder in order to reduce its oxidation and the morphology of Al powder was rod-like. The ratios of Ni to Al were fixed to be 1:1, 2:1, 3:1 (molar ratio, the following data are the same) and then they were dry mixed in a tri-dimensional (3-D) blender for about 6 h to produce a homogeneous powder mixture. Under axial pressure of 100 MPa, the mixtures were cold pressed into cylindrical compacts in a metal mold with dimensions of *d*20 mm×15 mm. The green disc-like compacts were put into a resistance furnace at 650 °C for 0.5 h for thermal explosion reaction. The products were then taken out and cooled down in the air.

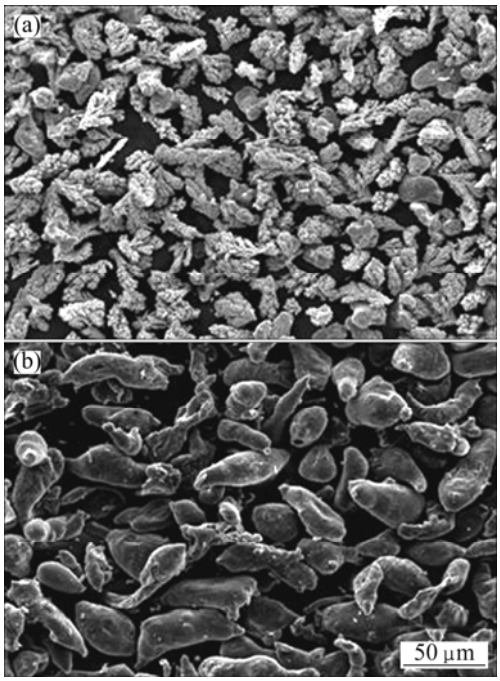

Fig. 1 SEM images of raw materials: (a) Ni powder; (b) Al powder

The samples cut from the products were characterized by X-ray diffraction (XRD, Model D/Max 2500PC Rigaku, Japan) to identify the crystalline phases. The samples for microstructure observation were prepared by conventional methods of mechanical polishing and chemical etching. The analyses of the microstructure and composition were performed by electron probe microanalysis (EPMA, JXA−8230). The microhardness values of different phases were measured by microhardness tester (FM−700) with a load of 0.49 N (50 gf) for 15 s.

3 Results

3.1 Phase analysis

Figure 2 shows the X-ray diffraction patterns of the products. It is indicated that a single NiAl phase is obtained with *n*(Ni):*n*(Al)=1:1. When the molar ratio of Ni to Al increases to 2:1, the phases in the product are composed of NiAl and Ni_3Al. In addition to the major phase NiAl, a small amount of Ni_3Al is formed. However, when the *n*(Ni):*n*(Al) increases to 3:1, the main phase in the product is Ni_3Al, and a small amount of NiAl is formed. This does not coincide with the phase constitution under equilibrium condition in Ni−Al phase diagram, which shows that a single Ni_3Al phase can be obtained with *n*(Ni):*n*(Al)=3:1 [15].

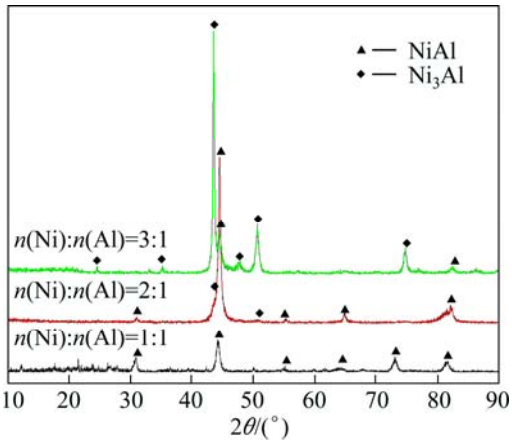

Fig. 2 XRD pattern of products with different molar ratios of Ni to Al

In addition, in the products with mole ratios of Ni to Al of 2:1 and 3:1, the diffraction peaks of NiAl deviate a

little at 2θ near 82° compared to 1:1 mole ratio product, as shown in Fig. 2. The causes will be analyzed together with phase composition later. Furthermore, it is obvious that the amount of NiAl phase decreases and Ni_3Al phase increases with increasing the Ni content.

3.2 Microstructure and microhardness

Figure 3 shows the images of microstructures of the

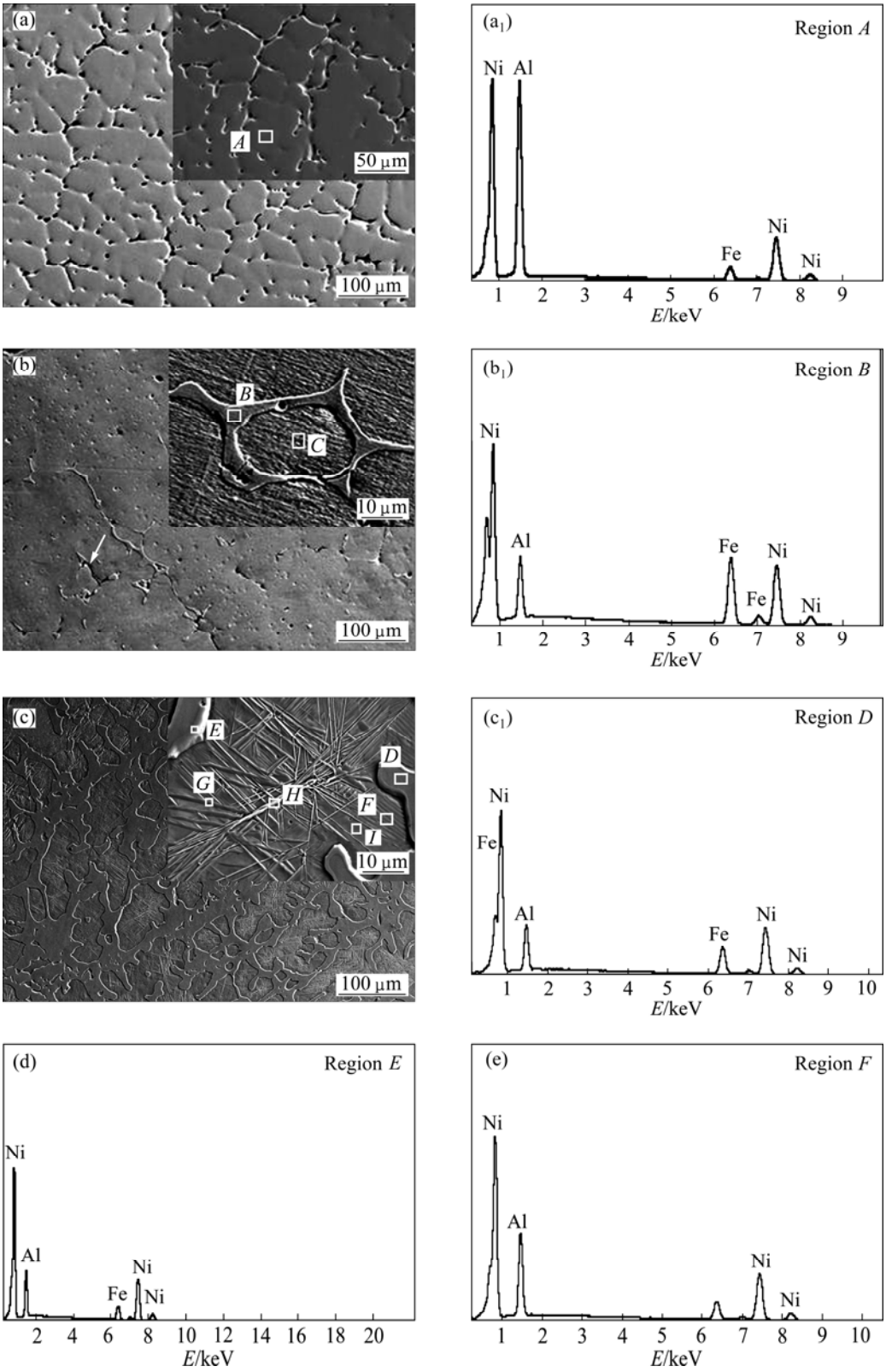

Fig. 3 SEM images (a, b, c) of microstructure and EDS spectra (a_1, b_1, c_1, d, e) corresponding to regions of products with different molar ratios of Ni to Al in powder: (a), (a_1) n(Ni):n(Al)=1:1; (b), (b_1) n(Ni):n(Al)=2:1; (c), (c_1), (d), (e) n(Ni):n(Al)=3:1

reaction products at low magnification and in detailed structural characters. The compositions of typical regions were measured by EDS and the results are shown in Table 1. As seen in Fig. 3(a), the sample of n(Ni):n(Al)= 1:1 has a uniform dendritic microstructure with some pores along the grain boundary, which may be deepened by chemical etching, and the composition of point *A* is Ni47−Al53 (molar fraction, %; the following data are the same), which is approximately to n(Ni):n(Al)=1:1, and its microhardness is about HV_{50} 358. Thus, it can be deduced that the uniform phases are single NiAl in accordance with the XRD analysis.

Table 1 Average chemical compositions of different regions corresponding to Fig. 3 analyzed by EDS

Region	x(Ni)/%	x(Al)/%	n(Ni)/n(Al)
A	47.27	52.73	0.89
B	78.07	21.92	3.56
C	66.67	33.33	2
D	78.95	21.05	3.75
E	75.06	24.94	3.01
F	67.63	32.37	2.09
G	70.50	29.50	2.39
H	71.67	28.33	2.53
I	67.26	32.74	2.26

In the sample of n(Ni):n(Al)=2:1, irregular precipitates along the grain boundaries of the matrix, in some places almost connecting to the network, can be observed clearly (see Fig. 3(b)). The EDS spectra of point *B* (precipitates at grain boundaries) and point *C* (matrix) show that the compositions are Ni78−Al22 and Ni67−Al33, respectively. And the average microhardness values of precipitates and matrix are HV_{50}369 and HV_{50}331, respectively. Consequently, combined with XRD analysis, it can be concluded that the irregular precipitates along the grain boundaries are Ni_3Al and the matrix is NiAl. In addition, some fine sub-structure characters in the matrix can be shown obviously upon high amplification. Calculated with the *K*-value method of X-ray diffraction, the relative contents of NiAl and Ni_3Al are 88.86% (mass fraction) and 11.14% (mass fraction), respectively.

With still further increasing n(Ni):n(Al) to 3:1, the microstructures of the sample are shown in Fig. 3(c). There are two kinds of constituents: one is irregular net-like structure in different thickness and shape, and its microhardness is HV_{50}354, similar to HV_{50}369 in region *B* in Fig. 3(b). Observation of the amplified image shows that there is no substructure in the grains but a continuous thin films covering on the margin. EDS analysis of regions *D* and *E* in Table 1 represent the composition of net-like structure and thin film, respectively. n(Ni):n(Al) values in both of the two parts are close to 3:1, although there is a slight difference between them. Thus, in association with the XRD results, it can be inferred that both the net-like structure and the thin film can be identified as Ni_3Al.

The other constituent in Fig. 3(c) is the remainder part which is surrounded by the irregular net-like structure and is called matrix. Upon amplified image, some substructures with different morphologies can be observed clearly. There are a great number of lath-shaped microstructures similar to the *M*-NiAl [18] (see the region *F*). However, twisted ridges (region *H*) with many radiating needle-like lines (region *G*) also exist in the center of the grain, which are not reported in other literatures. The Ni content of twisted ridges is 72%, which is approximate to 70.9% of Ni_3Al in Ref. [19], while the contents of Ni element in the needle-like and lath-shaped microstructures are 70% and 68%, respectively. It should be noted that the content of Ni element in these phases is clearly higher than the stoichiometric ratio of NiAl. Furthermore, the average microhardness of the matrix is HV_{50}560, which is higher than that in the β-NiAl phase in Figs. 3(a) and (b). Associated with XRD analysis, it can be concluded that the lath-shaped and the needle-like microstructures are *M*-NiAl and the twisted ridges are γ'-Ni_3Al. In addition, Fe exists in all the EDS spectra, which is most likely from the etching solution ($FeCl_3$ (5 g)+HCl (15 mL)+ alcohol (60 mL)).

4 Discussion

In this experiment, the green compact discs were put into a resistance furnace directly with a temperature of 650 °C. This may be equivalent to preheating the green compact to T_0=650 °C (923 K). Thus the highest reaction temperature T_{max} can be estimated by $T_{max}=T_0+T_{ad}$, where T_{ad} is the adiabatic combustion temperature. The T_{ad} values of NiAl and Ni_3Al are 1911 K and 1587 K [20], respectively. It can be suggested that the T_{max} would exceed the melting point T_m of NiAl and Ni_3Al. Consequently, once the reaction starts, the reaction rate is fast and in thermal explosion mode, and the NiAl and Ni_3Al phases would be melt immediately. This could also be supported by the melting phenomenon on the surface of the samples.

According to the Ni−Al phase diagram, when the molar ratio of Ni to Al is 1:1, only uniform NiAl with dendrite shape can be formed. When the molar ratio increases to 2:1, at the beginning of the cooling process, only uniform NiAl can be also formed, which is similar to n(Ni):n(Al)=1:1, especially at the high temperature

stage. However, due to the high content of Ni element, Ni_3Al will precipitate along the grain boundary of NiAl during the subsequent cooling process. In addition, according to the XRD analysis, the relative content of Ni_3Al is 11.14% (mass fraction), which is much lower than the content of Ni_3Al (46.02%, mass fraction) in equilibrium station determined by the lever rule. This results in the content of Ni in the matrix slightly higher than those under the equilibrium condition. Furthermore, during the whole reaction synthesis procedure, the intermediates such as Ni_5Al_3 could not be found. According to other literature [18], the phase should be formed by gradually heating to an appropriate temperature.

When the molar ratio of Ni to Al increases to 3:1, only Ni_3Al phases can be formed under the equilibrium cooling conditions, according to the Ni−Al phase diagram. In this experiment, although the temperature would exceed the melting point of NiAl and Ni_3Al could be melted partly, the ingredients are difficult to homogenize as the diffusion time is short and the melting is incomplete. At first, the primary β-NiAl phases would precipitate from the Al-rich liquid. As the temperature decreases below 1395 °C, the peritectic reaction $L+\beta\text{-NiAl}\longrightarrow\gamma\text{-Ni}_3\text{Al}$ occurs. Since the heating and holding time is short, the peritectic reaction could not proceed completely, thus, the remaining liquid directly transforms into Ni_3Al. The primary β-NiAl and γ-Ni_3Al are all non-equilibrium structures. Finally, the appearance of β-NiAl phases is coarse dendrites as the primary phase, whereas γ-Ni_3Al phases locate mainly at the grain boundaries of NiAl and in an irregular and net-like structure form, as shown in Fig. 3(c).

However, due to the volume shrinkage resulting from the liquid−solid transformation, small pores are formed in the grains of Ni_3Al and between the layer formed by peritectic reaction and the γ-Ni_3Al, as seen by the arrows in Figs. 4(a) and (b). Upon further rapid cooling, γ'-Ni_3Al would be precipitated from β-NiAl, and diversified morphology appears due to different positions and compositions. Some γ'-Ni_3Al phase forms along the grain boundaries of γ-Ni_3Al (see Fig. 4(b)). Some with pointed strip-like morphology string together as twisted ridges, and some distribute in the grains or along the grain boundaries of β-NiAl, as shown in Figs. 4(c) and (d).

With the formation of γ'-Ni_3Al, a great amount of stress would be generated around the γ'-Ni_3Al phases at high speed [21], especially at the tips of the pointed strip-like ones, due to the differences in structure between γ'-Ni_3Al (FCC) and β-NiAl (BCC). Hence, a lot of dislocations and twins may be formed on the interfaces between β and γ', γ and γ' [18]. This can induce β-NiAl to transform into M-NiAl with straight lath-like or radiating needle-like lines along the favorable growth orientation, as shown in Fig. 4(a).

Furthermore, due to the non-equilibrium cooling, the saturation of Ni in β-NiAl reaches 67.26% (molar fraction, marked I in Fig. 3(c)), which almost gets the maximum content of NiAl in Ni−Al diagram, especially at the position near the β-NiAl grain boundary. So, the diffusionless transformation of martensite would occur

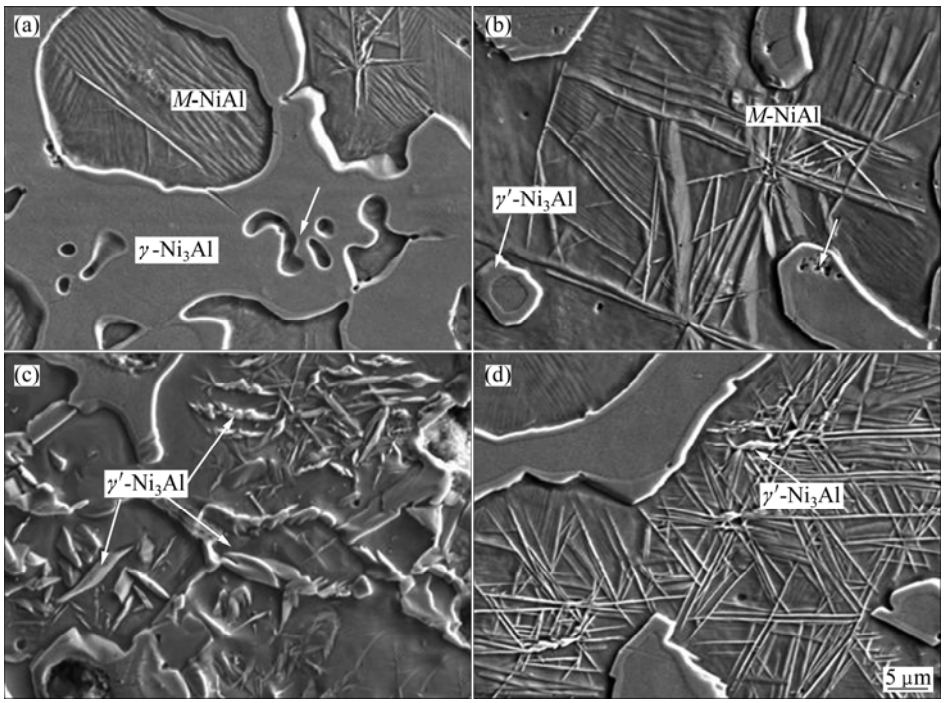

Fig. 4 SEM images of microstructure of products with n(Ni:)n(Al)=3:1 (molar ratio) showing different phases: (a) M-NiAl and γ-Ni_3Al; (b) M-NiAl and γ'-Ni_3Al; (c), (d) γ'-Ni_3Al

during the rapid cooling process [22]. Thus, a lot of fine and parallel lath bundle microstructures of *M*-NiAl with dislocations are observed on the grain edge of NiAl and the microhardness is clearly higher than that of the matrix of NiAl. In addition, with the molar ratio of Ni to Al of 2:1, parallel and lath-like substructures of *M*-NiAl are also observed in *β*-NiAl of the products, which demonstrates the effects of supersaturated Ni and the rapid cooling rate on the formation of *M*-NiAl again.

5 Conclusions

1) A single NiAl phase is obtained with the composition corresponding to the stoichiometric ratio of 1:1. However, the product is composed of the two-phase Ni_3Al+NiAl, when the molar ratios of Ni to Al increase to 2:1 and 3:1. In addition, as the Ni content increases, the contents of NiAl phases decrease while the contents of Ni_3Al phases increase.

2) With the molar ratio of 1:1, the sample has a uniform NiAl dendritic structure with some mesopores along the grain boundaries. By increasing the molar ratio to 2:1, the Ni_3Al phases precipitate along the grain boundaries of NiAl during the cooling process. And with the molar ratio of 3:1, the microstructures of the product become so complicated that lots of *M*-NiAl with needle-like or long lathing shape and many *γ*′-Ni_3Al with irregular and pointed strip-like morphology even appear besides *β*-NiAl with dendritic structure, *γ*-Ni_3Al with irregular or net-like morphology.

3) In the products of mole ratio of 3:1, with the precipitation of Ni_3Al in *β*-NiAl grains or along the grain boundaries during the cooling process, stress, dislocations and twins on the interfaces of Ni_3Al and *β*-NiAl sharply increase. This results in *β*-NiAl transforming into *M*-NiAl with parallel lath or radiating outward shapes. In addition, an excess of Ni and heterogeneity in the *β*-NiAl phase in rapid cooling also contribute to the formation of *M*-NiAl.

References

[1] DONG H X, HE Y H, JIANG Y, WU L, ZOU J, XU N P, HUANG B Y, LIU C T. Effect of Al content on porous Ni−Al alloys [J]. Materials Science and Engineering A, 2011, 528(13−14): 4849−4855.

[2] ISHIHARA S, KOISHI T, ORIKAWA T, SUEMATSU H, NAKAYAMA T, SUZUKI T, NIIHARA K. Synthesis of intermetallic NiAl compound nanoparticles by pulsed wire discharge of twisted Ni and Al wires [J]. Intermetallics, 2012, 23: 134−142.

[3] XU Gui-hua, WANG Guo-feng, ZHANG Kai-feng. Effect of rare earth Y on oxidation behavior of NiAl−Al_2O_3[J]. Transactions of Nonferrous Metals Society of China, 2011, 21(s2): s362−s368.

[4] DUARTE L I, LEINENBACH C, KLOTZ U E, MARKER M C J, RICHTER K W, LOFFLER J F. Experimental study of the FeAl−NiAl−TiAl section [J]. Intermetallics, 2012, 23: 80−90.

[5] OZDEMIR O, ZEYTIN S, BINDAL C. Tribological properties of NiAl produced by pressure-assisted combustion synthesis [J]. Wear, 2008, 265(7−8): 979−985.

[6] WANG Zhen-sheng, XIE Yi, GUO Jian-ting, ZHOU Lan-zhang, HU Zhuang-qi, ZHANG Guang-ye, CHEN Zhi-gang. High temperature oxidation behavior of directionally solidified NiAl−31Cr−2.9Mo−0.1Hf−0.05Ho eutectic alloy [J]. Transactions of Nonferrous Metals Society of China, 2012, 22(7): 1582−1587.

[7] ZHU S Y, BI Q L, NIU M Y, YANG J, LIU W M. Tribological behavior of NiAl matrix composites with addition of oxides at high temperatures [J]. Wear, 2012, 274−275(27): 423−434.

[8] XIE Yi, GUO Jian-ting, ZHOU Lan-zhang, CHEN Hong-dong, LONG Yi. Microstructural evolution and mechanical properties of new multi-phase NiAl-based alloy during heat treatments[J]. Transactions of Nonferrous Metals Society of China, 2010, 20(12): 2265−2271.

[9] SUN Bao-de, YANG Gen-cang, ZHOU Yao-he, LIN Dong-liang. The rapidly solidified microstructure of NiAl intermetallic compound [J]. Chinese Journal of Material Research, 1996, 10(3): 267−270. (in Chinese)

[10] COLIN J, SERNA S, CAMPILLO B, FLORES O, JUAREZ-ISLAS J. Microstructural and lattice parameter study of as-cast and rapidly solidified NiAl intermetallic alloys with Cu additions [J]. Intermetallics, 2008, 16: 847−853.

[11] PABI S K, MURTY B S. Mechanism of mechanical alloying in Ni−Al and Cu−Zn systems [J]. Materials Science and Engineering A, 1996, 214(1−2): 146−152.

[12] RUIZ-LUNA H, ALVARADO-OROZCO J M, CACERES-DIAZ A, LOPEZ-BAEZ I, MORENO-PALMERIN J, ESPINOZA-BELTRAN F J, BOLDRICK M S, TRAPAGA-MARTINEZ G, MUNOZ-SALDANA J. Structural evolution of B_2−NiAl synthesized by high-energy ball milling [J]. Journal Materials Science, 2013, 48(1): 265−272.

[13] DONG H X, JIANG Y, HE Y H, SONG M, ZOU J, XU N P, HUANG B Y, LIU C T, LI P K. Formation of porous Ni−Al intermetallics through pressureless reaction synthesis [J]. Journal of Alloys and Compounds, 2009, 484(1−2): 907−913.

[14] OZDEMIR O, ZEYTIN S, BINDAL C. A study on NiAl produced by pressure-assisted combustion synthesis [J]. Vacuum, 2010, 84(4): 430−437.

[15] BISWAS A, ROY S K. Comparison between the microstructural evolutions of two modes of SHS of NiAl: Key to a common reaction mechanism [J]. Acta Materialia, 2004, 52(2): 257−270.

[16] FAN Q C, CHAI H F, JIN Z H. Dissolution–precipitation mechanism of self-propagating high-temperature synthesis of mononickel aluminide [J]. Intermetallics, 2001, 9: 609−619.

[17] ZHU P, LI J C M, LIU C T. Reaction mechanism of combustion synthesis of NiAl [J]. Materials Science and Engineering A, 2002, 329−331: 57−68.

[18] CHENG T Y. On annealed Ni−34.6 at% Al at 1523 K and effects of cooling rates [J]. Journal of Materials Science, 1995, 30(11): 2877−2887.

[19] KANG H J, WU S K, WU L M. Martensitic transformation of $Ni_{64}Al_{34}Re_2$ shape memory alloy [J]. Intermetallics, 2010, 18: 123−128.

[20] MORSI K. Review: Reaction synthesis processing of Ni−Al intermetallic materials [J]. Materials Science and Engineering A, 2001, 299(1−2): 1−15.

[21] HANGEN U D, SAUTHO G. The effect of martensite formation on the mechanical behaviour of NiAl [J]. Intermetallics, 1999, 7: 501−510.

[22] THOMPSON R J, ZHAO J C, HEMKER K J. Effect of ternary elements on a martensitic transformation in *β*-NiAl[J]. Intermetallics, 2010, 18(5): 796−802.

反应合成 Ni−Al 金属间化合物的组织及形成机理

崔洪芝，魏 娜，曾良良，王晓彬，汤华杰

山东科技大学 材料科学与工程学院，青岛 266590

摘 要：以 Ni 粉和 Al 粉为原料，通过热爆反应合成制备 Ni−Al 系金属间化合物，研究了反应物摩尔比对生成物物相、组织结构和显微硬度的影响。结果表明：当 Ni、Al 摩尔比为 1:1 时，反应生成物为单一的 NiAl 相；当 Ni、Al 摩尔比为 2:1 时，生成物相组成为 NiAl+Ni_3Al 相，因为非平衡冷却，NiAl 含量多，呈不规则块状形态分布，Ni_3Al 相析出量少，主要沿初生 NiAl 晶界分布，当进一步提高 Ni 含量，且 Ni、Al 摩尔比为 3:1 时，生成物组织形态复杂，除枝晶状的 β-NiAl、粗大块状和网状的 γ-Ni_3Al 外，还有板条状和针片状的 *M*-NiAl 和不规则的块状或者尖条状的 γ'-Ni_3Al，这主要是由非平衡冷却和 β-NiAl 内的成分差异而引起的。

关键词：金属间化合物；Ni−Al；反应合成；显微组织

(Edited by Hua YANG)